Failure analysis of a high-speed offset bearing

Daniela M.BUZESCU
INCDT COMOTI
Senior researcher
Bucharest ROMANIA
daniela.buzescu@comoti.ro

Sorin Gabriel TOMESCU
INCDT COMOTI
Senior researcher

ABSTRACT

There are presented the consequences of the events during the operation of two variants of sliding bearings (offset type) within two gearboxes of similar construction and way of loading. Both assemblies have suffered serious damages of the gear transmission (gear teeth breaking, active flanks scoring, etc.), accidents that occurred after a longer or shorter period of use. During operation, each gearbox was monitored and the parameters values were recorded: gas turbine speed, driving power, important temperatures (oil input, bearing surface, etc.), vibrations (proximity sensor on the input shaft, accelerometer on the gearbox housing). For each type of bearing, the geometric characteristics are presented, the antifriction material is described by its mechanical properties, and the dynamic characteristics of the bearing surface are used to estimate the critical mass which establishes the boundary between stable and unstable operation. Relying on the operating parameters, the behaviours of two HS bearings (HS Sun pinion bearings), which have been analysed are compared mainly during instability occurrences and especially in the last period before their removal from service. The conclusion is that the stability of the undamaged fluid film bearing is proved both from the computational model and by the dynamic response of bearing to external loading.

KEYWORDS: offset-halves bearing, high speed, low load, vibration, cavitation erosion,

NOMENCLATURE

Bxx, Bxy, Byx, Byy	Damping coef. [N s/m];
C_L	Machined clearance of lobe [mm];
C_B	Bearing clearance [mm];
D_B	Bearing diameter [mm];
D_L	Lobe diameter [mm];
D_S	Shaft diameter [mm];
e	Eccentricity[mm];
e_x	Shaft displ. normal to load direction [mm];
e_y	Shaft displ. in direction of load [mm];
h_{min}	Minimum film thickness [μm];
H	Power loss [kW];
HS	High speed;
Kxx, Kxy, Kyx, Kyy	Stiffness coefficient [N/m];
L	Length [mm];
M_c	Critical mass, [kg];
m	Preset ($m=1-c_B/c_L$);
n	Rotational speed [rpm];
O_j	Journal centre;
O_L	Lower-lobe centre;
O_U	Upper-lobe centre;
p_{med}	Specific load [Mpa];
t	Normal operating temperature [°C];
t_{IBA}	Input bearing alarm point [°C];
Q	Rate of oil flow [l/min];
v_{IBA}	Vibration alarm point [m/s] (filtered – measured on casing);
v	Sliding speed [m/s];
W	Load [N];
α	Asymmetry coefficient;
2xβ	Bore type [arc degrees];
δ	Offset [mm];
Δt	Rise of oil temperature [°C];
Θ	Angle measured from horizontal split axis; in direction of rotation [deg]
ω	Angular velocity of shaft [rad/s];
Φ	Attitude angle [deg];
Phase I	Normal operation
Phase II	Beginning of failure

Phase III End of operation

1 INTRODUCTION

This paper presents the analysis of the high-speed bearings damage, specifically failures of a type of planetary gear set ('Compound Star' type Epicyclic Speed Reducing gearbox – 1.8 MW), which makes the connection between the gas turbine (drive turbine – 19000 rpm) and the electric generator (driven machine – 1500 rpm). In the gearbox construction, the input shaft is supported by a single bearing – a sliding bearing – and transmits the motion from the drive turbine to the planet gears (the first stage of planetary gear used to reduce the engine speed).

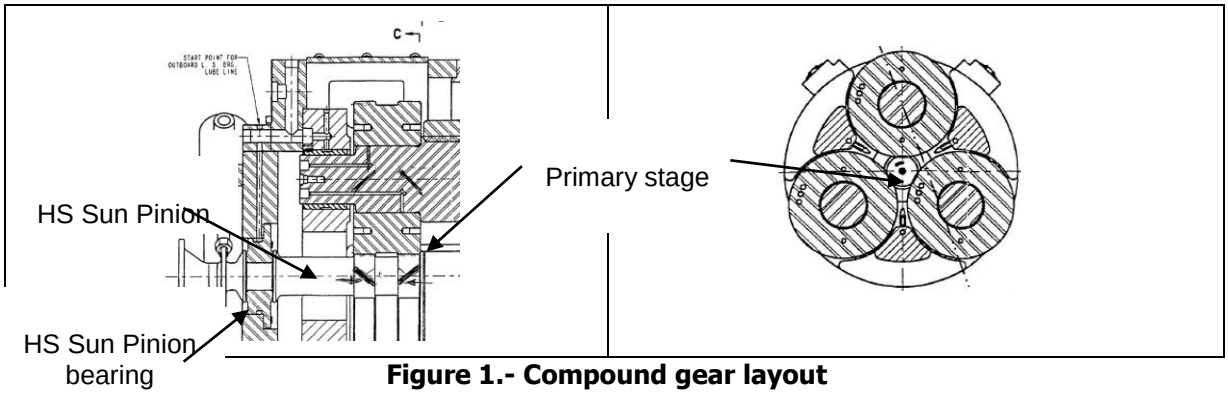

Figure 1.- Compound gear layout

The two examined gearboxes, whose operation came to an end along with the destruction of the inlet bearing, are similar in terms of construction and loading. The behaviour of the HS Sun Pinion Bearing variants has been monitored during the entire time of use.
The novelty of this research consists in conducting, relying on in-situ experiments, of a new study on offset bearings, slightly loaded and subjected to high operating speeds.

2 THEORETICAL ANALYSIS

2.1 Bearing profile

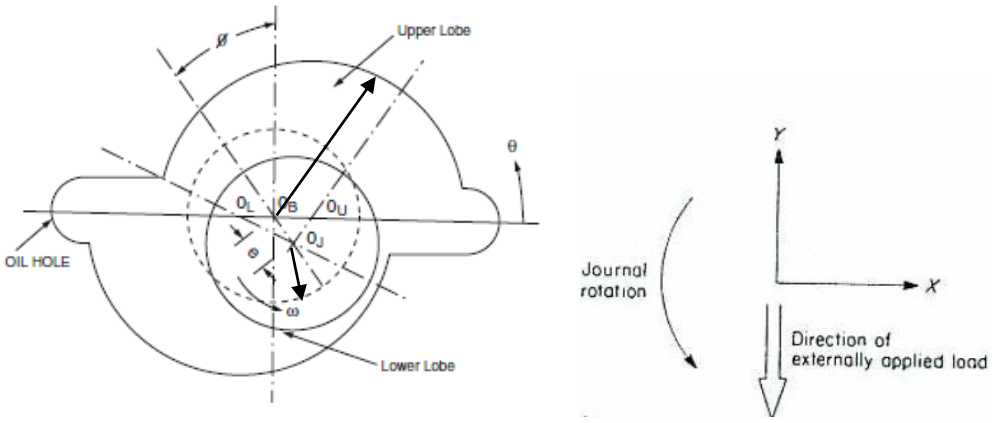

Figure 2. Schematic diagram of offset-halves journal bearing [1;3]

Figure 2 presents the section of an offset-halves bearing. Two oil grooves of 30 degrees exist at the angles of θ=0° and θ=180°. X and Y are the horizontal and respectively the vertical coordinates.
Offset-halves journal bearings have the durability equal to lemon bore bearings, but the former bearings have good stiffness and damping properties, which enables light loads while bearing runs at high speed (figure 3).

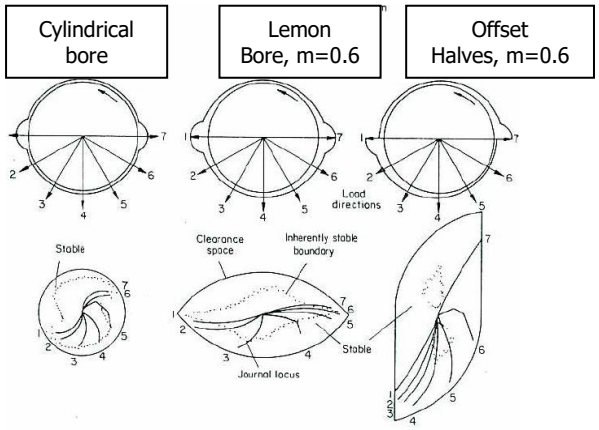

Figure 3 – Regions of inherent stability for variously profiled bore bearings (m-preset) [1]

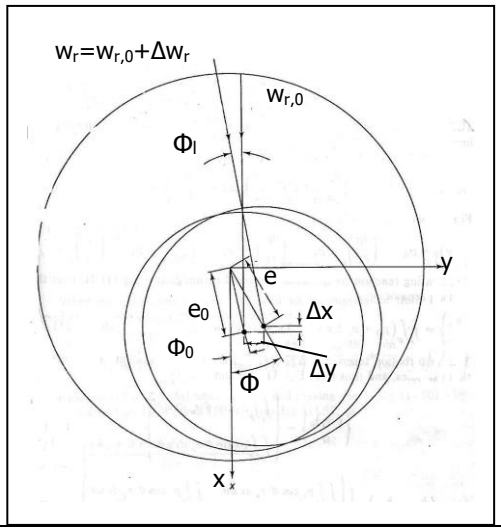

Figure 4. – Effect of changing the load on bearing's shaft position and relevant parameters associated with these changes

2.2 Stability of the bearing spindle

Considering the mass of the shaft (m_a) and bearing's shaft position (subscript 0 refers to quasi-steady state position, Δx and Δy are the displacements of the shaft from this position -fig. 4)

$e_0 \cos\Phi_0 + \Delta x = e\cos\Phi$ and $e_0 \sin\Phi_0 + \Delta y = e\sin\Phi$ (1)

The equation of motion (*from* [9]) for the journal may be written as:

$$\begin{Bmatrix} m_a & 0 \\ 0 & m_a \end{Bmatrix} \frac{\partial^2}{\partial t^2} \begin{Bmatrix} e\cos\phi \\ e\sin\phi \end{Bmatrix} = \begin{Bmatrix} w_r\cos\phi_l \\ w_r\sin\phi_l \end{Bmatrix} - \begin{Bmatrix} (w_x)_0 \\ 0 \end{Bmatrix} \quad (2)$$

The assumption of small amplitude motions about an equilibrium position allows in expressing the bearing reaction forces as a Taylor Series expansion around the static journal position:

$$w_x = (w_x)_0 + \left(\frac{\partial w_x}{\partial x}\right)_0 \Delta x + \left(\frac{\partial w_x}{\partial y}\right)_0 \Delta z + \left(\frac{\partial w_x}{\partial \dot{x}}\right)_0 + \left(\frac{\partial w_x}{\partial \dot{y}}\right) \quad (3)$$

$$w_y = (w_y)_0 + \left(\frac{\partial w_y}{\partial x}\right)_0 \Delta x + \left(\frac{\partial w_y}{\partial y}\right)_0 \Delta z + \left(\frac{\partial w_y}{\partial \dot{x}}\right)_0 + \left(\frac{\partial w_y}{\partial \dot{y}}\right) \quad (4)$$

Recall that the direction of the x axis was chosen so that $(w_y)_0 = 0$. Letting

$$b_{xx} = \left(\frac{\partial w_x}{\partial \dot{x}}\right)_0 \quad b_{xy} = \left(\frac{\partial w_x}{\partial \dot{y}}\right)_0 \quad b_{yx} = \left(\frac{\partial w_y}{\partial \dot{x}}\right)_0 \quad b_{yy} = \left(\frac{\partial w_y}{\partial \dot{y}}\right)_0$$

$$k_{xx} = \left(\frac{\partial w_x}{\partial x}\right)_0 \quad k_{xy} = \left(\frac{\partial w_x}{\partial y}\right)_0 \quad k_{yx} = \left(\frac{\partial w_y}{\partial x}\right)_0 \quad k_{yy} = \left(\frac{\partial w_y}{\partial y}\right)_0$$

allows eqs.(3) and (4) to be expressed as

$$\begin{Bmatrix} w_x \\ w_y \end{Bmatrix} = \begin{Bmatrix} (w_x)_0 \\ 0 \end{Bmatrix} + \begin{Bmatrix} k_{xx} & k_{xy} \\ k_{yx} & k_{yy} \end{Bmatrix} \begin{Bmatrix} \Delta x \\ \Delta y \end{Bmatrix} + \begin{Bmatrix} b_{xx} & b_{xy} \\ b_{yx} & b_{yy} \end{Bmatrix} \begin{Bmatrix} \Delta\dot{x} \\ \Delta\dot{y} \end{Bmatrix} \quad (5)$$

By substituting equation (5) into equation of motion (2), it is obtained:

$$\begin{Bmatrix} m_a & 0 \\ 0 & m_a \end{Bmatrix}\begin{Bmatrix} \Delta\ddot{x} \\ \Delta\ddot{y} \end{Bmatrix} + \begin{Bmatrix} b_{xx} & b_{xy} \\ b_{yx} & b_{yy} \end{Bmatrix}\begin{Bmatrix} \Delta\dot{x} \\ \Delta\dot{y} \end{Bmatrix} + \begin{Bmatrix} k_{xx} & k_{xy} \\ k_{yx} & k_{yy} \end{Bmatrix}\begin{Bmatrix} \Delta x \\ \Delta y \end{Bmatrix} = \begin{Bmatrix} w_r\, cos\Phi_l \\ w_r\, \sin\Phi_l \end{Bmatrix} - \begin{Bmatrix} (w_x)_0 \\ 0 \end{Bmatrix} \tag{6}$$

Considering a stationary load ($w_r = w_{x,0}$, $\Phi_l = 0$), the linearized equation of journal motion reduces to:

$$\begin{Bmatrix} m_a & 0 \\ 0 & m_a \end{Bmatrix}\begin{Bmatrix} \Delta\ddot{x} \\ \Delta\ddot{y} \end{Bmatrix} + \begin{Bmatrix} b_{xx} & b_{xy} \\ b_{yx} & b_{yy} \end{Bmatrix}\begin{Bmatrix} \Delta\dot{x} \\ \Delta\dot{y} \end{Bmatrix} + \begin{Bmatrix} k_{xx} & k_{xy} \\ k_{yx} & k_{yy} \end{Bmatrix}\begin{Bmatrix} \Delta x \\ \Delta y \end{Bmatrix} = \begin{Bmatrix} 0 \\ 0 \end{Bmatrix} \tag{7}$$

The eight dynamic coefficients are functions of the bearing's operating parameters only, which are characterized by the static equilibrium eccentricity ratio and the attitude angle. Thus, the linearization of the bearing reaction forces has the evident advantage of decoupling the rotor and the bearing. The stiffness and damping coefficients can be made dimensionless by the following equations (offset halves bearings' damping coefficients -b_{xy} and b_{yx} -are symmetric but stiffness coefficients are not) :

$$\begin{Bmatrix} K_{xx} & K_{xy} \\ K_{yx} & K_{yy} \end{Bmatrix} = \frac{c}{w_r}\begin{Bmatrix} k_{xx} & k_{xy} \\ k_{yx} & k_{yy} \end{Bmatrix} \quad \begin{Bmatrix} B_{xx} & B_{xy} \\ B_{yx} & B_{yy} \end{Bmatrix} = \frac{c\omega}{w_r}\begin{Bmatrix} b_{xx} & b_{xy} \\ b_{yx} & b_{yy} \end{Bmatrix} \tag{8}$$

By solving equation (7), it is shown that under certain circumstances a non-trivial solution exists. The solution is of the type:

$$\begin{Bmatrix} \Delta x \\ \Delta y \end{Bmatrix} = \begin{Bmatrix} x_h \\ y_h \end{Bmatrix} \exp\left(\bar{\Omega} t\omega\right) \tag{9}$$

Substituting equation (9) into equation (7) gives:

$$\begin{Bmatrix} M_a + \bar{\Omega}B_{xx} + K_{xx} & \bar{\Omega}B_{xy} + K_{xy} \\ \bar{\Omega}B_{yx} + K_{yx} & M_a + \bar{\Omega}\mathrm{B_{yy}} + \mathrm{K_{yy}} \end{Bmatrix}\begin{Bmatrix} x_h \\ y_h \end{Bmatrix} exp(\bar{\Omega} t\omega) = \begin{Bmatrix} 0 \\ 0 \end{Bmatrix} \tag{10}$$

Where $M_a = \dfrac{cm_a\bar{\Omega}}{w_r}$ and $\bar{\Omega} = \dfrac{\Omega}{\omega}$

Thus the result which can be obtained is either $x_h = y_h = 0$ (trivial steady-state solution) or

$$(M_a + \bar{\Omega}B_{xx} + K_{xx})(M_a + \bar{\Omega}B_{yy} + K_{yy}) - (\bar{\Omega}\mathrm{B_{yx}} + \mathrm{K_{yx}})(\bar{\Omega}\mathrm{B_{xy}} + \mathrm{K_{xy}}) = 0 \tag{11}$$

The solution given in eq. (11) is an eigenvalue problem stating that if the system would dislodge itself from the steady-state position, a transient vibration will result although the external load is constant.

The eigenvalue $\bar{\Omega}$ will generally be complex such as: $\bar{\Omega} = -\bar{\Omega}_d + i.\bar{\Omega}_v$ (12)

The transient shaft motion will be:

$$\begin{Bmatrix} \Delta x \\ \Delta y \end{Bmatrix} = \begin{Bmatrix} x_h \\ y_h \end{Bmatrix} \exp(-\bar{\Omega}_d t\omega)[\cos(\bar{\Omega}_v t\omega) + i.\sin(\bar{\Omega}_v t\omega)] \tag{13}$$

where x_h and y_h are also complex.

The left term of eq. (13) is real, so that only the real part of the right side will be necessary to describe the physical motion. The value of $\bar{\Omega}$ (and $\bar{\Omega}_d$) will be obtained from eq. (11). It is noteworthy that when $\bar{\Omega}_d > 0$, the shaft displacement away from equilibrium position will decrease continuously, since xh and y_h are constants, and finally reach the steady-state position. Such a behaviour is obviously stable if those deviations from steady-state conditions disappear due to the damping action of hydrodynamic film. When $\bar{\Omega}_d < 0$, the shaft vibration will increase and will be restricted only by the bearing sleeve. The "threshold of instability" occurs at $\bar{\Omega}_d = 0$. Substituting eq. (12) into eq. (11) results in two equations, the first one being for the real part and the second one for

the imaginary part. At the threshold of instability, $\overline{\Omega}_d = 0$, the second equation for imaginary part results in:

$$(M_a)_{cr} = (\frac{cm_a\omega^2}{w_r})(\overline{\Omega}_v)^2_{cr} = \frac{B_{xx}K_{yy} + B_{yy}K_{xx} - B_{yx}K_{xy} - B_{xy}K_{yx}}{B_{xx} + B_{yy}} \quad (14)$$

Using the first equation for the real part, at the threshold of instability ($\overline{\Omega}_d = 0$), it is obtained:

$$(\overline{\Omega}_v)^2_{cr} = \frac{[K_{xx} - (M_a)_{cr}][K_{yy} - (M_a)_{cr}] - K_{xy}K_{yx}}{B_{xx}B_{yy} - B_{xy}B_{yx}} \quad (15)$$

If M_a is smaller than $(M_a)_{cr}$, the system will be stable ($\overline{\Omega}_d > 0$), but it will be unstable for M_a larger than $(M_a)_{cr}$. Thus, the bearing's susceptibility to instability obviously depends on the values of the bearing coefficient, which in its turn depends on the bearing type and its various specific parameters.

3. BEARING DATA

The input shaft bearing is low loaded (supporting the weight force of the input shaft and the coupling flanges, and a possible unbalanced force of planet gears which mate with the sun gear-). The sun gear has a very high speed, being directly driven by the gas turbine at 19000 rpm. The oil type being used was ISO VG 32, oil inlet temperature was 60 - 68 °C;

3.1 The first gearbox

The first transmission: the gearbox documentation includes the HS Sun Pinion bearing technical data
Load = 228 [N];
Oil Filtration Level = 10 microns;
Bearing Material: steel backed, Anti-friction coating: Babbitt (88%Sn, 8%Sb, 4%Cu); (t=20°C, hardness 17-24 HV-SR ISO 4383, allowable compressive stress–14N/mm^2); coating thickness: >1mm;
Weight of HS Sun Pinion assembly: 18.6 kg (14.1kg- HS Sun Pinion; 4.5kg – coupling).

Table 1. Geometric Data

D_B [mm]	L [mm]	L/D	$2c_B$ [mm]
50	40	0.8	0.1143-01397

Table2. Operating Data

t[°C]	p_{med} N/m2]	v[m/s]	t_{IBA} [°C]	v_{IBA}[m/s]
60-85	0.114	49.6	104	0.01016

Table 3. Stiffness and Damping Coefficients

Kxx·10^3 [N/m]	Kxy·10^3 [N/m]	Kyx·10^3 [N/m]	Kyy·10^3 [N/m]
43081.166232	20489.822964	-93342.526836	39403.505700
Bxx [N s/m]	**Bxy [N s/m]**	**Byx [N s/m]**	**Byy [N s/m]**
32048.184636	-19614.189504	-19614.189504	77931.377940

The results of calculations give: $(M_a)_{cr} = 8.02$ and ($\overline{\Omega}_d > 0$), thus $M_a = 5.115 < (M_a)_{cr}$, the bearing is not susceptible to instability when operation is carried out in steady-state conditions.

3.2 The second gearbox

For the second transmission, the documentation includes technical data [*from* 6].
Load / Load direction: 228 N/ behind centre of pad;
Oil Filtration Level = 5 microns;

Bearing Material: Bearing body: C15; Anti-friction coating: Babbitt 738 (81.3%Sn, 12%Sb, 6%Cu; 0.6%Zn;**0.1%Ag**) (Hardness: 20°C – 26HB; Compressive stress–yield point 87 N/mm^2), coating thickness: >1 mm;
Weight of HS Sun pinion assembly: 18.6 kg (14.1kg- HS Sun Pinion; 4.5kg – coupling).

Table 4. Geometric Data

D_B [mm]/ D_S [mm]	L [mm]	L/D	2xβ	δ [mm]	$2c_B$ [mm]
$60^{+0.019}$ /59.874 $_{-0.013}$	40	0.7	2x150°	0.040	0.126- 0.142

Table 5. Operating Data – Calculation Results

t [C]	p_{med} [N/m2]	V [m/s]	t_{IBA} [°C]	v_{IBA} [m/s]	e_x/ e_y [mm]	h_{min} [mm]	Δt [°C]	H [kW]	Q [l/min]
57	0.095	59.6	104	0.0102	0.003 0.001	0.060	10	3.66	12.86

Table 6. Stiffness and Damping Coefficient

Kxx ·10^3 [N/m]	Kxy·10^3 [N/m]	Kyx·10^3 [N/m]	Kyy·10^3 [N/m]
16882.2	-21628.1	66099.5	57224.8
Bxx [N s/m]	**Bxy [N s/m]**	**Byx [N s/m]**	**Byy [N s/m]**
22100	1400	1400	80800

The results of the stability computations for the high-speed bearing are: $(M_a)_{cr} = 6.892$ and $(\overline{\Omega}_d > 0)$, thus $M_a = 3.442 < (M_a)_{cr}$, that means the bearing is not susceptible to instability when operating in steady-state conditions.

4 MONITORING

The operation control was achieved by the following several parameters: input speed, turbine power (in generator mode power percentage – 106%), oil and bearing temperatures, input pinion shaft vibrations, and global vibration measured on the casing with an accelerometer. Proximity measurement is a more precise method in vibration analysis
Temperatures were measured at the inlet of the oil in the gearbox and with sensors, measuring bearing body temperature, placed in close proximity to the active surface of the bearing.
Vibration monitoring was carried out both on the input shaft with proximity transducer (displacements - of microns) and with accelerometer on the reducer assembly casing, monitoring speed [mm/s].
The parameter "turbine power" is actually the electric generator power percentage – 106% and its values are affected by the electric factors (the power factor), so it does not reflect the operating variations of the gearbox.
The recordings made during the normal operation (phase I), at the onset of the fault (phase II) and then before the stop (phase III), are shown for each transmission in turn.
A brief description of the event is presented for each transmission in order to make a comparison between the severity of the accident and the level of destruction of the high speed bearing.

4.1 The first gearbox

The first transmission has had an operation time of 37,670 h [7]. Damage occurred as a result of incorrect gear mesh between the input pinion and the planetary gears: the double helical planet gears worked only on left-hand side helical teeth; supplementary, one of the planets had an important misalignment between its own rotation axis and sun gear pinion axis. As a result of the gear overload, an input shaft tooth fragment broke (fig. 4 [7]) and the second reduction stage was damaged. The input shaft spindle shows normal wear traces (fig.4), The occurrence of the vibration peaks recorded by the proximity sensor during the last 1500 h of operation shows an alteration in the operation of the bearing, although the difference between the inlet oil temperature and the temperature of the bearing has remained about 10° C. After these signs appeared, the planetary transmission was still kept in operation for about 2 months (1500 h) before the failure occurred.

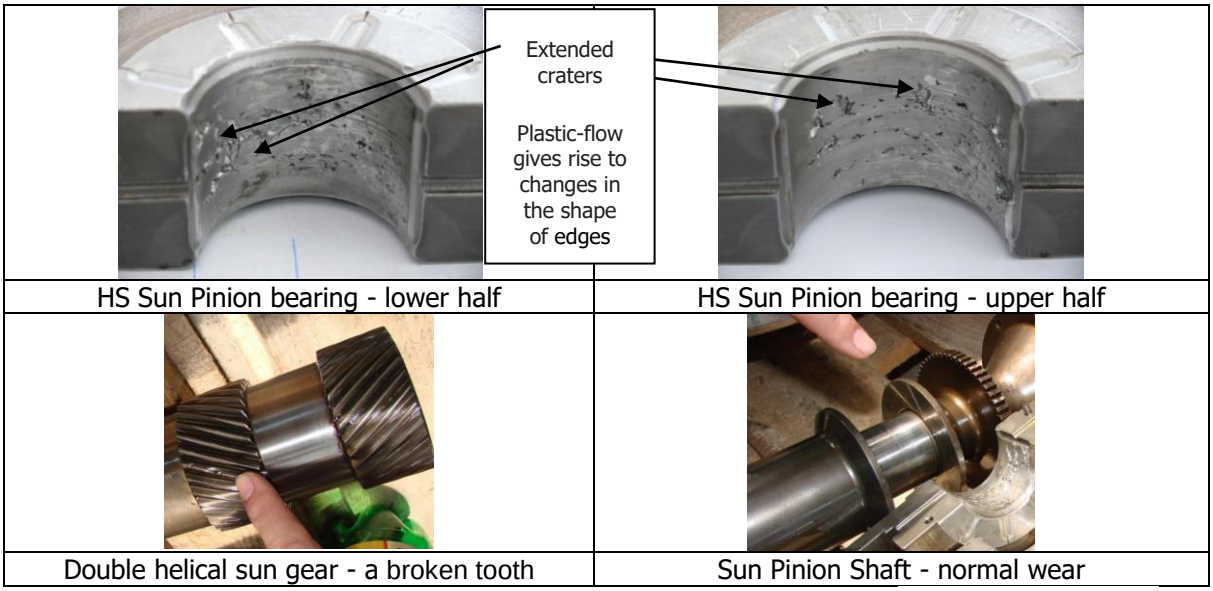

Figure 4 - First transmission - HS Sun Pinion - Bearing and Shaft reaching the end of their life [7]

Phase I - Vibration recordings (see the first transmission charts) on the sun pinion shaft and on the gear case during normal operation show a relatively stable operation (40-50μm and 1.5 - 2 mm/s).
Phase II is marked by increased vibrations recorded by the proximity transducer on the input shaft (from 50 μm to 60 μm with peaks of up to 70 μm) and recorded on the gear case (from 2.5 mm/s to 3.5 mm/s with peaks up to 5 mm/s). Starting from this phase, with the disequilibrium of the gears that are in mesh, it is interesting to observe that the aspect of the vibrations recorded by the proximity sensor is very closely followed by the aspect of the vibrations recorded by the accelerometer on the case. Thus it may be concluded that the main instability source is in the input shaft gear, instability that is transmitted to the assembly. However, between the vibration high values, there are intervals of time in which the bearing operates in quasi-stable regime.
Phase III - the onset of damage to HS sun pinion bearing: the higher level vibration has damaged the bearing surface (micro-cavitation failure has occurred - macro and micro-debris detached from the bearing surface, higer specific pressure - anti-friction coating flowing in the direction of movement), the material damages widened, which increased the instability and has further contributed to the increase in vibrations. As stated above, in the last recordings (phase III) as well, the occurrence of vibrations increase on the gear case closely follows the aspect of the vibrations recorded on the input shaft, it can be concluded that the bearing itself has become a source of instability and, hence, the acceleration of its own damage is proven.

4.2 The second gearbox

The second gear speed reducer had an operation time of 1500 hours, between 21.07-30.12.2011, (with a stop operation of about two months due to an overhaul of the whole plant [8]) On dismantling, the visual inspection of the input shaft revealed a totally different aspect of the double helical gear. The left-hand side of the helical gear (shaft end) was still undamaged, whilst the right-hand side of the helical gear was broken. The occurrence of the bearing failure was a micro-fatigue damage (cavitation erosion - surface fatigue failure) as well (Fig. 5) the subsequent - multiple-point detachment of anti-friction coating, as a result of high frequency vibrations. This bearing had a much better behaviour at the specific pressure resulting from the vibrations, the coating surface showing multiple scratches and craters but no material detachment occurrence over large areas, although the dynamic load level was high (see the second transmission charts).
Phase I – (the input shaft vibrations increase beginning with the first operating cycles). The vibrations recorded by the proximity transducer indicate a completely unstable operation from the very beginning, but which is not transmitted to the gearbox assembly–the recordings of the accelerometer are not identical to the ones of the proximity sensor. The instability manifests only at the level of the Sun pinion shaft, as a consequence of the unbalance of the gearing triangle. Only one planet of

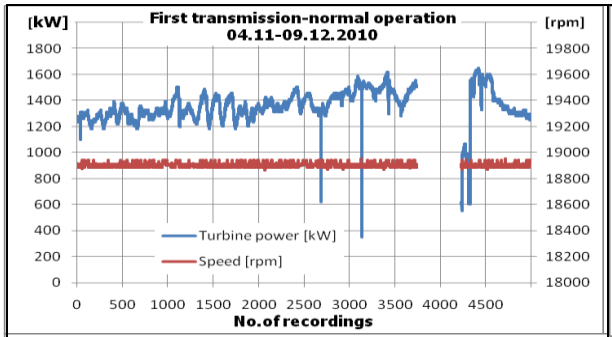

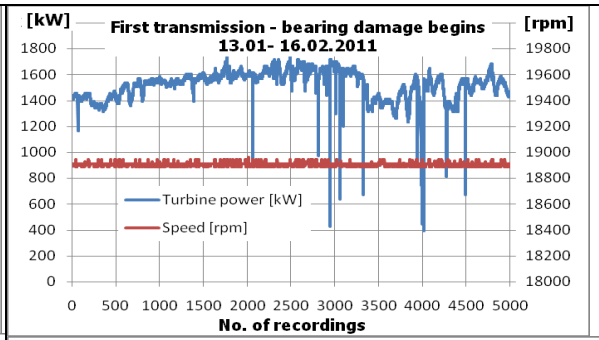

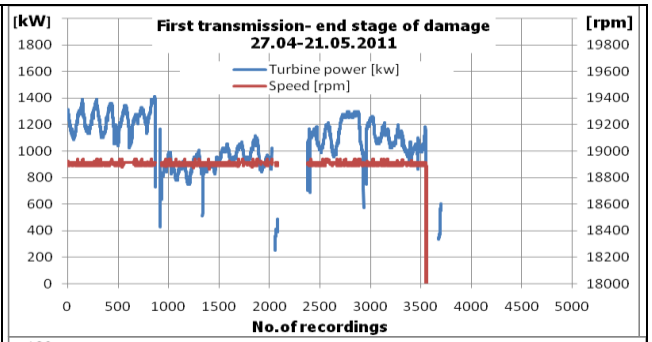

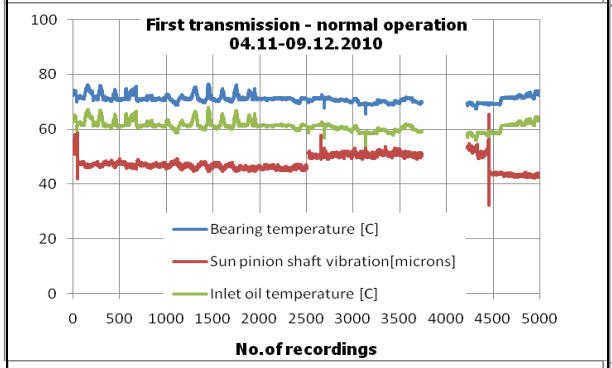

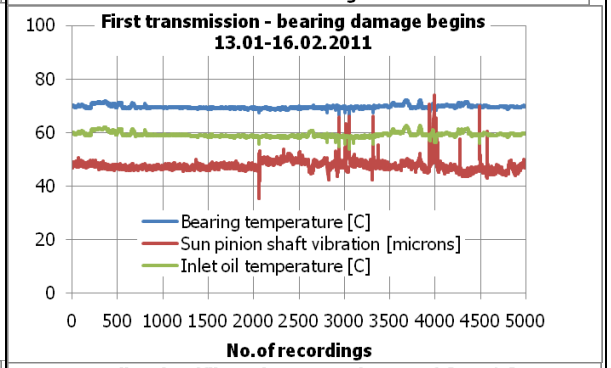

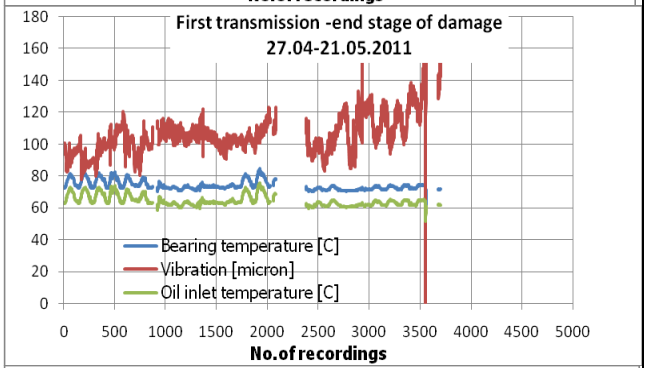

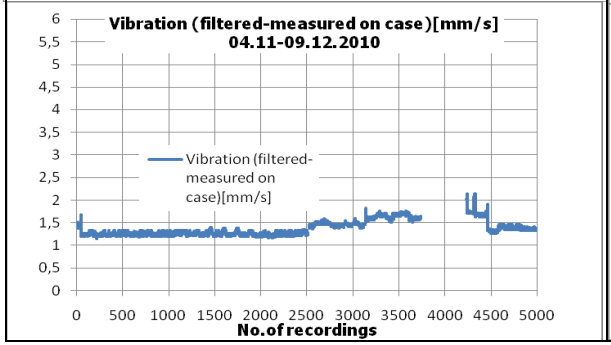

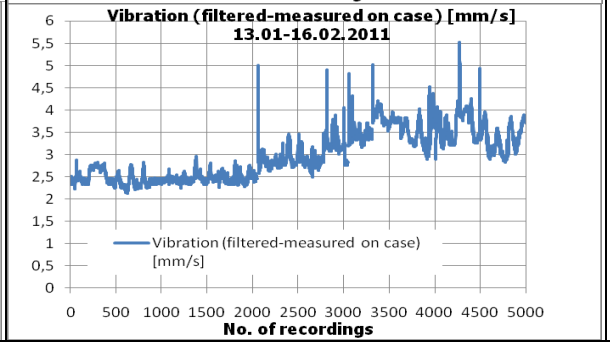

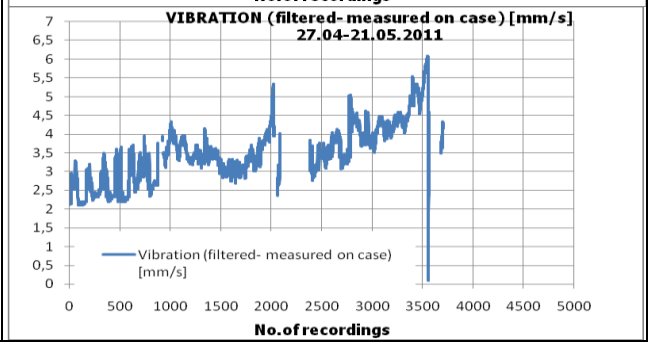

NOTE: 1-Sampling rate is one recording at 10 min; 2- the chart contains a gap in a line - the data range contains a blank cell - meaning "operation was stopped

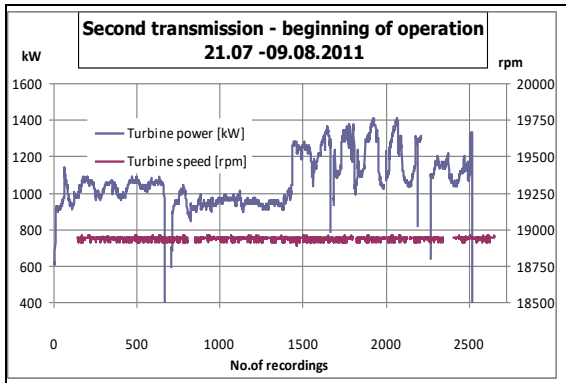

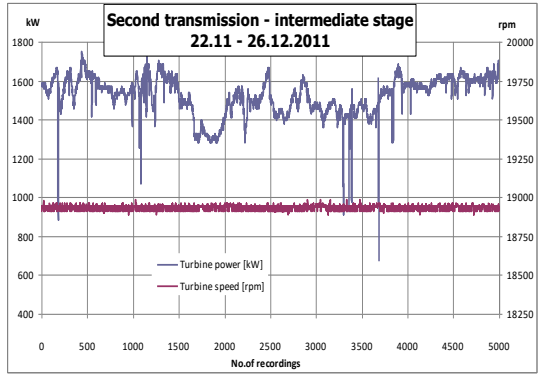

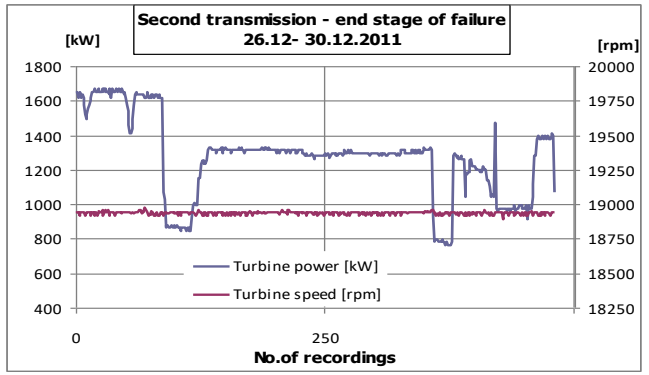

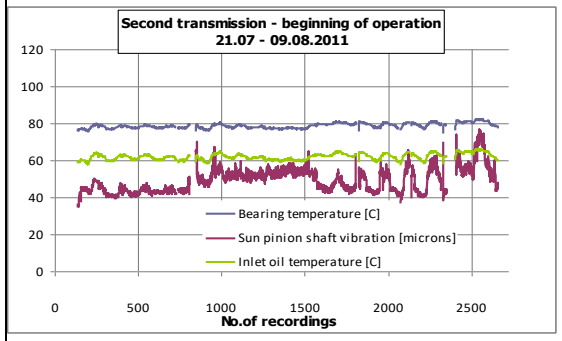

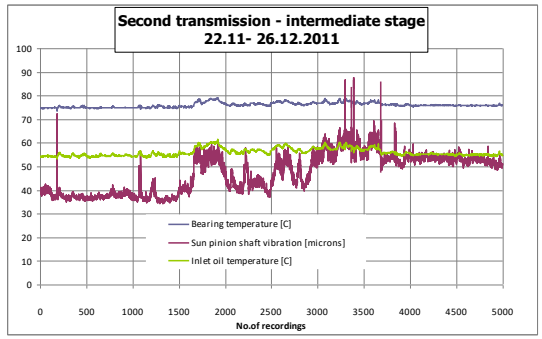

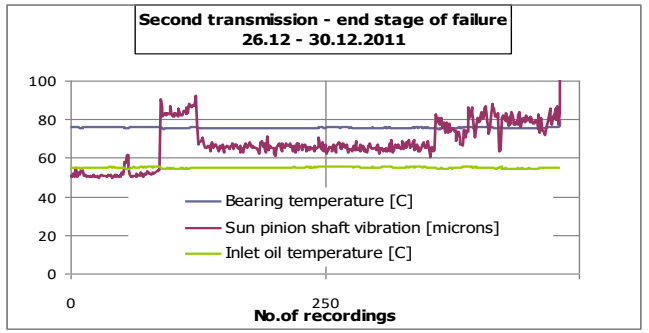

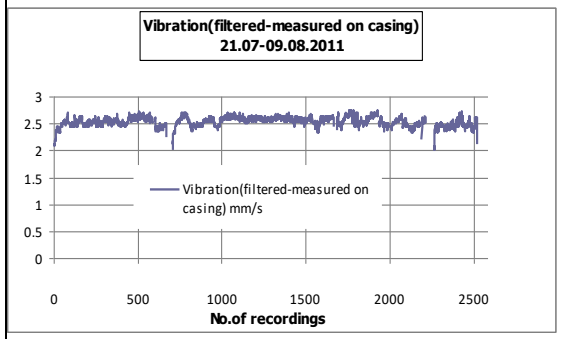

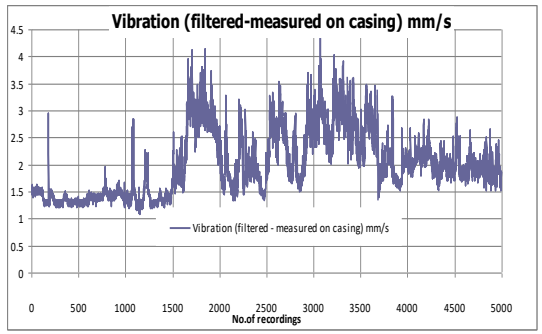

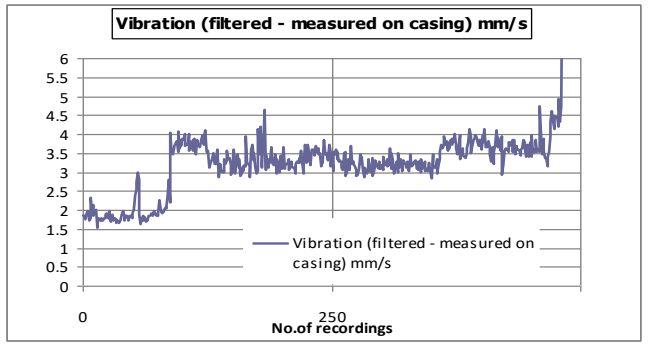

NOTE: 1-Sampling rate is one recording at 10 min; 2- the chart contains a gap in a line - the data range contains a blank cell - meaning "operation was stopped

	
Offset bearing - cavitation erosion	Right-hand side of the helical gear broke

Figure 5 - Second transmission - HS Sun Pinion - Bearing and Shaft -1500 h of operation

the first gear stage (gear teeth meshing process) was most probably the cause of bearing instability.
Phase II - the bearing instability increases. The vibrations recorded on the case increased significantly especially in the second part of the phase. The dynamic loadings appear as shocks which are recorded by the proximity sensor on the input shaft (teeth begin to break on one side of the V of the first gear stage) and the vibrations are amplified of the entire mass of the gearbox assembly. In the last part, between the shocks, the proximity vibrations do not stabilize, the dynamic loading exceeds the capacity of the bearing damping.
Phase III – It can see, the right-hand side of the helical gear was broken, whilst the left-hand side remained undamaged. The operation of the input shaft is marked by less often shocks, which alternate with stability intervals. In the end, the damages of the anti-friction surface manifests in the rise of vibrations amplitude up to the break down limit. Again, it is observed the very high resemblance between the aspects of the recordings on the input shaft and on the case, as a consequence of the influence of the input shaft.
Similarly to the first transmission, the increase in the temperature recorded in the bearing does not change during operation (all the time, the difference has remaining at around 20°C)

5 CONCLUSIONS

By comparing the bearings behaviour in the two cases, it can be concluded:

- the dynamic characteristics of the bearings show good stability in quasi-stationary conditions-unbalanced gear forces are causes of the beginning bearing failure
- the damping of undamaged bearing has a large effect on rotor stability: the mechanical shocks (as shown by vibration peaks) are followed by the return to lower amplitude vibration, to its quasi steady state regime.
- in both cases, the periods of accentuated instability recorded with the proximity sensor, are approximately equal (approx. 1500 h);it is obvious that the bearing of the first transmission has a higher damage degree: the antifriction material compressive strength is approximately 2.5 times lower than antifriction material compressive strength for the second transmission; on the damaged bearing surface the material has yielded on the edge of the craters, although there are no changes in temperature rise

REFERENCES

1. Garner,D.R., Lee, C.S ,.Martin F.A *Stability of profile bore bearings: influence of bearing type selection*, WAUKESHA bibliography, LB 456/80;
2. Pascovici, M.D., Cicone, T *"Elemente de tribologie"*, Cursuri universitare, Editura BREN, Bucuresti 2002 (Elements of tribology - Bren University yextbook, Publishing House BREN)
3. Chauhan Sehgal R. *"Classification of Non-circular Journal Bearings",* Springer Briefs, 2016
4. Constantinescu, V.N. Nica Al., Pascovici M.D, Ceptureanu Gh., Nedelcu St. - *"Lagăre cu Alunecare"* Ed.Tehnica, Bucuresti, 1980 (Sliding bearings, Publishing House TEHNICA, Bucharest, 1980)
5. Barwell, F.T., Lingard, S. *"The thermal equilibrium of plain journal bearings",* Proceedings of the 6th Leeds-Lyon Symposium on Tribology, Sept. 18-21, 1979. Mech. Engn. Publ., London, 1980
6. Crane J - Offset-halves-calculation, Calculation results LB6054a1_1, 29-May-2008
7. Raport tehnic final PHILADELPHIA
8. Raport tehnic 103-reductor COMOTI
9. Hamrock B.J.- *"Fundamentals of fluid film lubrication"* McGraw-Hill,Inc, New York